Exact diagonalization of finite frustrated spin-$\frac{1}{2}$ Heisenberg models

F. Figueirido
Institute for Theoretical Physics, State University of New York at Stony Brook, Stony Brook, New York 11794

A. Karlhede
Institute for Theoretical Physics, University of Stockholm, Vanadisvägen 9, S-11346 Stockholm, Sweden

S. Kivelson* and S. Sondhi
Department of Physics, State University of New York at Stony Brook, Stony Brook, New York 11794

M. Rocek
Institute for Theoretical Physics, State University of New York at Stony Brook, Stony Brook, New York 11794

D. S. Rokhsar†
IBM Research Division, Thomas J. Watson Research Center, P.O. Box 218, Yorktown Heights, New York 10598
(Received 20 January 1989)

We have studied the spectrum of low-spin eigenstates of a spin-$\frac{1}{2}$ Heisenberg model on 4×4 square lattices with up to third-neighbor antiferromagnetic exchange interactions. We have computed the staggered susceptibility, spin-spin correlation function, and the overlap of the exact ground state with various variational spin-density-wave ordered states as well as with the equal-amplitude, nearest-neighbor resonating-valence-bond state (which is the prototypical short-ranged RVB state). We find evidence for a complicated phase diagram with a region in which a short-ranged RVB state may be the ground state.

I. INTRODUCTION

The notion that the ground state of a sufficiently frustrated spin-$\frac{1}{2}$ Heisenberg model may be disordered (a "quantum spin liquid") plays a prominent role in several theories[1-7] of the origin of superconductivity in highly correlated two-dimensional electron gases. Frustration appears to be necessary to stabilize a spin-liquid state, since most studies[8-11] of unfrustrated antiferromagnetic Heisenberg models have concluded (although not rigorously proved) that the ground state has nonzero long-range antiferromagnetic order.

One can classify the possible ground states of quantum spin systems by their broken symmetry and excitation spectra. For the purposes of this paper it is useful to consider a partial catalog.

(i) A spin-density-wave (or Néel) state, which we denote SDW, has broken translational, spin-rotational, time-reversal, and parity symmetry. Independent of the value of the microscopic spin, the low-energy excitations of this ordered state are spin-1 gapless "Goldstone" modes, or magnons.

(ii) A spin-Peierls state (or valence-bond crystal) has broken translational symmetry without broken spin-rotational symmetry. It has a severalfold degenerate ground state, and a gap in its excitation spectrum. We expect that all the excitations of a spin-Peierls state have integer spin.

(iii) A spin-liquid state is translationally and spin rotationally invariant. There are several possible subclasses of spin liquid states. (It remains to be established which of them, if any, exist as the ground state of a sensible spin model.) We distinguish a *compressible* from an *incompressible* spin liquid depending on whether or not there is a gap to spin excitations. We draw a further distinction between an *integer* spin liquid, in which all finite energy quasiparticles have integer spin, and a *half-integer* spin liquid, which possesses finite energy half-integer spin excitations. Since our primary interest is in the spin-liquid states, we briefly list some proposed liquid states.

(a) There exist exactly soluble models in arbitrary dimension with integer spin per unit cell which can be shown to have unique, disordered ground states with a nonzero gap.[12] Presumably, as suggested by single-mode analysis and numerical studies of one-dimensional chains, these are examples of incompressible integer-spin liquids.

(b) The short-ranged resonating-valence-bond (SR-RVB) state,[2,4] of which the prototypical example[13] is the nearest-neighbor RVB state (NN-RVB), is an incompressible spin liquid. This state corresponds closely to the chemist's picture[14] of resonating valence bonds. It has been suggested that the excitations of a SR-RVB state are spin-$\frac{1}{2}$ "spinons," although it remains unclear whether or not they are generically confined. An example of a particular exactly soluble model with a SR-RVB ground state is the Klein model, discussed in the following.

(c) Recently,[15] one of us has argued that, viewed as a spin system, a BCS s-wave superconductor is an example of an incompressible half-integer spin liquid. Transla-

tional symmetry is unbroken, although, of course, gauge invariance is broken. There is a gap to spin excitations, and the lowest-energy spin excitations (the Bogoliubov quasiparticles) are neutral fermions which carry spin $\frac{1}{2}$. Indeed, the SR-RVB state is essentially a Gutzwiller projected fully gapped BCS state.[1]

(d) Incompressible spin-liquid states may break time-reversal invariance. For instance, Kalmeyer and Laughlin[4] have proposed a state based on an analogy with the fractional quantum Hall effect which has broken time-reversal symmetry.[16] Such a state is thought to have half-integer spin excitations with fractional statistics.

(e) Compressible spin-liquid states with gapless spin excitations can also be envisioned. Examples of these "long-ranged" RVB states are the ground state of the spin-$\frac{1}{2}$ nearest-neighbor antiferromagnetic chain, and the ground states of certain two-dimensional SU(N) antiferromagnets in the large-N limit. These latter states have $S=\frac{1}{2}$ quasiparticle excitations with either a pseudo-Fermi surface[1] or pseudo-Fermi points.[6,7]

(f) Ioffe and Larkin[17] have shown that for a large spin ($S \gg 1$) frustrated Heisenberg antiferromagnet, there exists a narrow region of parameter space [of width of order $\exp(-S)$] in which there exists a spin-liquid phase (presumably of the incompressible integer-spin variety). Chakravarty, Halperin, and Nelson[10] have also suggested, based on hydrodynamic arguments relating the long-wavelength properties of the antiferromagnet to the properties of a $(2+1)$-dimensional nonlinear σ model, that as a function of increasing frustration there could be a second-order transition from a SDW (Néel) state to a quantum-paramagnetic state, which in this language is an integer spin, incompressible spin liquid.

This list is certainly not exhaustive; even more exotic states are possible, such as valence-bond liquid crystal states, which break the point-group symmetry of the lattice but are translationally and spin rotationally invariant,[18] or Wiegmann[19] states which break specific combinations of time-reversal and translational symmetry.

The Klein model[20,21] is a spin-$\frac{1}{2}$ Heisenberg model which is known not to have a SDW ground state. It has an extensive ground-state entropy; the ground-state manifold is spanned by the set of nearest-neighbor valence-bond (NN-VB) states. Any superposition of NN-VB states (and only such a state) is a zero-energy ground state of H_K. The Klein Hamiltonian, H_K, is equal to the sum over all sites of the projection operator onto the highest spin state of the total spin on that site and its nearest neighbors. On a square lattice, this model has competing first-, second-, and third-neighbor antiferromagnetic exchange interactions in the ratio $J_1:J_2:J_3=1:1:0.5$, as well as short-ranged four-spin interactions. Any small perturbation about the Klein model will select a particular superposition of NN-VB's to be the ground state (up to a possible degeneracy of order 1 in the thermodynamic limit). Which superposition is selected depends on the nature of the perturbation. Thus, the Klein model is at a multicritical point in Hamiltonian space. Each of these superpositions is believed to have an exponentially decaying spin-spin correlation function[5] and a gap in its spin-excitation spectrum. In Ref. 3 (see also Appendix B) it was shown that the properties of a weakly perturbed Klein model at energies small compared to the spin gap are equivalent to those of a hard-core quantum-dimer gas, in which the dimer is roughly representative of a valence bond. From an approximate analysis of this model, it was concluded that a NN-RVB state would have a branch of low-lying spin-0 excitations, dubbed "resonons."

The fact that the Klein model has exact NN-VB ground states suggests, more generally, that sufficiently frustrated spin-$\frac{1}{2}$ Heisenberg models may have SR-RVB ground states. Here we report the results of exact diagonalization studies of finite-size models with first (J_1), second (J_2), and third (J_3) neighbor antiferromagnetic exchange interactions, in a modest attempt to test the validity of this suggestion. We were largely motivated in this study by the success of similar studies[22] for the fractional quantum Hall effects: As in that case, one expects that results for finite-size systems may give reliable evidence for the existence of an incompressible liquid phase, since unless the system is near a critical point such a state should have a correlation length of order one lattice constant. Of course, because the systems we have studied are small, we cannot be confident that all of the behavior described below is representative of the system in the thermodynamic limit. We note, however, that the NN-RVB state is known to have a short correlation length (about 1.3 lattice constants[11]). Given the existence of a SR-RVB phase, our system should be large enough so that our conclusions are self-consistent. With these caveats, we feel our results lend support to the notion that frustrated spin-$\frac{1}{2}$ Heisenberg models can have SR-RVB ground states.

In summary, our numerical study has led us to three major interferences concerning the effect of frustration on the thermodynamic states of a spin-$\frac{1}{2}$ Heisenberg antiferromagnet. We list them in order of decreasing certainty: (a) There exists a parameter range of the (highly) frustrated Heisenberg model which has a non-SDW ground state, i.e., the ground state does not spontaneously break spin-rotational symmetry. (b) In the non-SDW region of the phase diagram, there exists a region in which the ground state is a liquid; the ground state does not have spontaneously broken translational symmetry (i.e., spin-Peierls order). (c) In the liquid phase, there exists a region where the overlap with the nearest-neighbor RVB state is large, and where the spectrum and correlation functions behave as expected of a SR-RVB state. This suggests that there exists a liquid phase which is adiabatically related to the nearest-neighbor RVB state, and which can reasonably be identified as a SR-RVB phase. We return to these points in Sec. IV.

In Sec. II we explicitly describe the calculations we have performed. In Sec. III we give the results of those calculations with a minimum of interpretation. In Sec. IV we outline our three major conclusions, which follow from these results and certain plausible assumptions which are detailed below. Finally, we briefly comment on the relevance of this result to the theory of high-temperature superconductivity. In Appendix A we discuss the analytic solution to the same problem on a small-

er (eight-site) lattice. In Appendix B, we discuss the relation between the putative spin-liquid phase and the quantum hard-core dimer gas.

II. DESCRIPTION OF THE CALCULATIONS

The calculations are conceptually straightforward. Consider a 4×4 square lattice with either periodic boundary conditions (PBC's), or twisted boundary conditions (TBC's) which are periodic in the y direction but "twisted" in the x direction, so that the site $(1,n)$ is taken to be a nearest neighbor of the site $[4, n+2(\text{mod } 4)]$. Both boundary conditions are chosen so that they do not frustrate any of the candidate ground states. By comparing the results from these two sets of boundary conditions, we can to some extent monitor finite-size effects and sensitivity to boundary conditions.

The Hamiltonian is block diagonalized by classifying the states according to the irreducible representations of the total spin rotation group (i.e., by their total spin S and the total z component of the spin S_z), and the translational group whose irreducible representations are labeled by an index $\mathbf{k}$. In the case of PBC's, $\mathbf{k}$ is the crystal momentum, $\mathbf{k}=(k_x,k_y)$, where $k_i=0$, $\pm\pi/2$, or π. For TBC, $\mathbf{k}=(k,\nu)$, where $\nu=\pm1$ depending on whether the state is odd or even under reflection about the x axis, and $\mathbf{k}=0$, $\pm\pi/4$, $\pm\pi/2$, or π, is the x component of the crystal momentum. The TBC's have the advantage that they allow a larger number of distinct values of $\mathbf{k}$, so we have been more thorough in our study of the system with these boundary conditions. In addition, while for both boundary conditions, the number of distinct first and second neighbors of a site is the same as for the infinite system, for TBC's each site has three distinct third-nearest neighbors while for PBC's it has only two. Because of this difference, in comparing results for the two boundary conditions, we rescale J_3 such that $(J_3)^{\text{PBC}}=(\frac{3}{2})(J_3)^{\text{TBC}}$ (see also Appendix A).

Once the Hamiltonian is block diagonal, the blocks are diagonalized numerically. The largest block is 105×105 (TBC) and 107×107 (PBC) in the spin-0 sector and 218×218 (TBC) in the spin-1 sector. The eigenenergies and eigenstates can then be compared with various variational states. We solved the model analytically along the line $J_1=0$, and the results constitute a check of our numerical computations (see Appendix A).

To obtain a qualitative understanding of our numerical results, one can consider the energy of various candidate variational ground states. A NN-RVB variational ansatz for the ground state was obtained by taking the equal amplitude superposition of all nearest-neighbor valence-bond states with phases determined by Marshall's criterion.[23] The energy of this NN-RVB state (obtained from its spin-spin correlation function on a 4×4 lattice[5]) is

$$E_{\text{NN-RVB}}\approx-0.33J_1+0.15J_2+0.15J_3\ . \quad (1)$$

Three variational spin-density-wave states ($|\text{SDW}_1\rangle$, $|\text{SDW}_2\rangle$, and $|\text{SDW}_3\rangle$) were also considered, where $|\text{SDW}_i\rangle$ is the ground state for $J_i=1$ and $J_k=0$ for $k\neq i$: $|\text{SDW}_1\rangle$ is the ground state of the nearest-neighbor Heisenberg model, which presumably has long-ranged order of the sort shown in Fig. 1(a) in the limit of a large

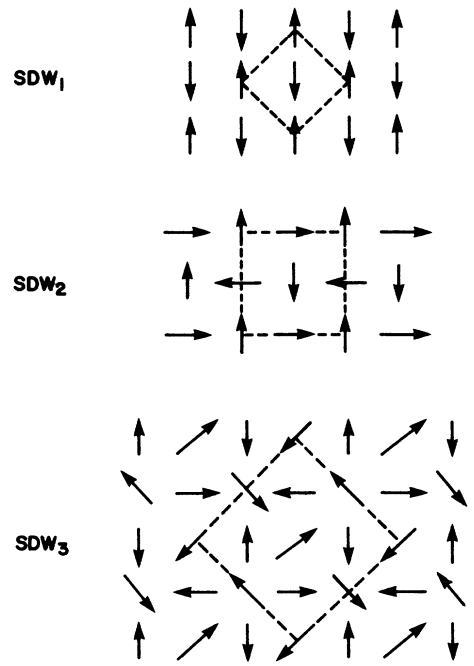

FIG. 1. Schematic renditions of the long-ranged magnetic order inferred for the states referred to in the text as (a) SDW_1, (b) SDW_2, and (c) SDW_3. At the classical level, the energy is independent of the relative angle between the axes of quantization on the different sublattices; the results of our first-order spin-wave analysis and evidence (see Fig. 4) from our numerical calculations suggest that this decoupling of the lattices survives quantum corrections. This implies that these states would have more than the Goldstone mode with zero energy.

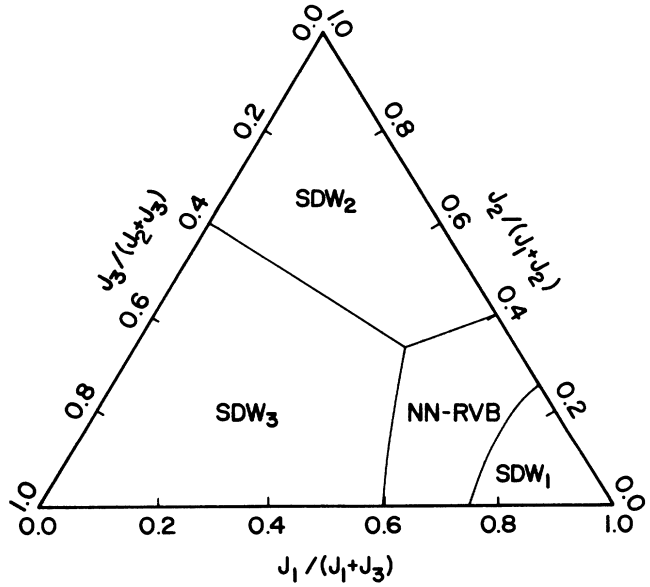

FIG. 2. Analytic estimates of the phase diagram in the thermodynamic limit, obtained as described in Eqs. (1) and (2) in the text. Compare with Figs. 3(a) and 3(b).

system, and $|\mathrm{SDW}_2\rangle$ and $|\mathrm{SDW}_3\rangle$ consist, respectively, of two and four interpenetrating versions of $|\mathrm{SDW}_1\rangle$ on different sublattices, as shown in Figs. 1(b) and 1(c). Theoretical estimates for the ground-state energy per spin of these SDW states can be obtained by computing the spin-spin correlation functions in each state SDW_i on a 4×4 lattice. For these states, this gives the following estimates for the ground-state energy:

$$
\begin{aligned}
E_{\mathrm{SDW1}} &\approx -0.35J_1+0.21J_2-0.21J_3\ , \\
E_{\mathrm{SDW2}} &\approx 0.00J_1-0.35J_2+0.21J_3\ , \\
E_{\mathrm{SDW3}} &\approx 0.00J_1+0.00J_2-0.35J_3\ .
\end{aligned}
\tag{2}
$$

The energy estimates of Eqs. (1) and (2) yield approximate phase boundaries for the frustrated Heisenberg model studied here. The results are shown in Fig. 2. As can be seen in the figure, these rather naive estimates

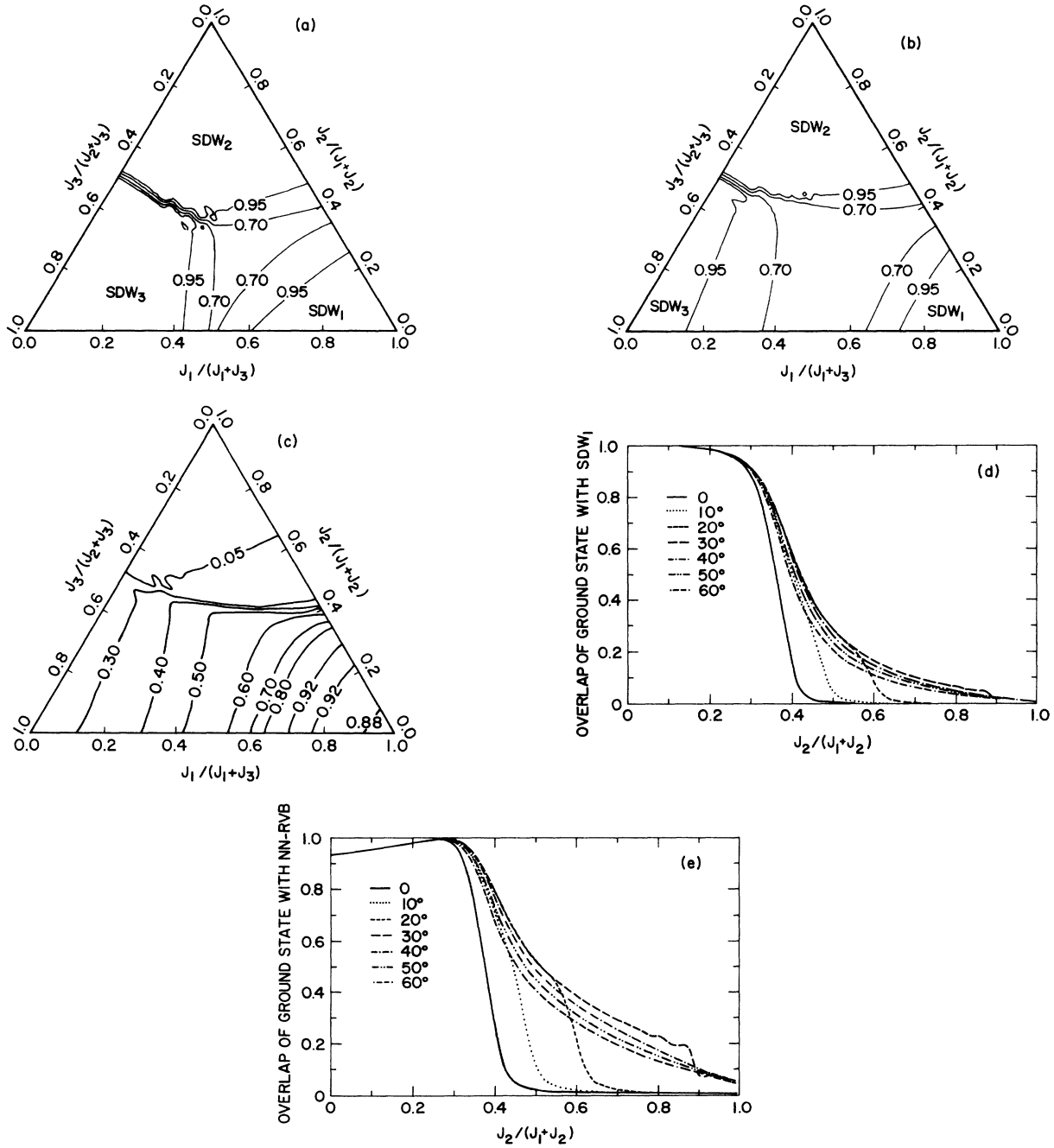

FIG. 3. Plots of the overlap between the exact ground-state wave function and the various variational wave functions defined in the text: (a) and (b) show the 95% and 70% overlap contours with SDW_i (a) for PBC's and (b) for TBC's. (c) shows a contour map of the overlap with NN-RVB for TBC's. The corner labeled J_1 corresponds to $J_2=J_3=0$, and similarly for the remaining corners, with J_1 normalized so that they add up to 1 everywhere. The small-scale structures are artifacts of the interpolation. (d) Overlap with the SDW_1 states for TBC's as a function of J along lines radiating out at 10° intervals from the J_1 corner, starting from the $J_3=0$ line. (e) Similar plot for the overlap with NN-RVB.

coincide fairly well with the regions where the character of the ground state is changing (as determined by where the state with the largest overlap changes—see Fig. 3 below). A sophisticated spin-wave calculation[24] with $J_3=0$ also suggests the existence of an intermediate phase or phases between SDW_1 and SDW_2. For $|SDW_2\rangle$, as J_1 and J_3 are made different from zero, the classical ground-state energy will be independent of the relative orientation of the staggered magnetization of the two interpenetrating SDW's. Similarly, for $|SDW_3\rangle$ at the classical level, the four interpenetrating SDW's can have any relative orientation. Ioffe and Larkin[17] have argued that for the classical Heisenberg model with $J_3>0$, a helicoid state is favored for $J_1<2J_2+4J_3$. (We find this phase is stable for $2J_2+4J_3>J_1>2J_2-4J_3$.) Our system is too small to accommodate an incommensurate SDW.

III. RESULTS

A. Results of the numerical experiments for twisted boundary conditions

(1) Even for the simple nearest-neighbor antiferromagnetic Heisenberg model ($J_1:J_2:J_3=1:0:0$), where the ground state is thought to have long-ranged SDW order, the equal amplitude NN-RVB state has[25] overlap

$$|\langle \text{NN-RVB}|\Psi_0\rangle|=0.93=(0.9954)^{16}$$

with the exact ground-state wave function $|\Psi_0\rangle$. This is a remarkably large overlap for a 16-spin system and a zero parameter variational wave function. For generic approximate ground states, even very good ones, we expect the overlap with the true ground states to fall exponentially with the number of sites, so a better figure of merit might be the 16th root of the overlap. For example, the overlap with the classical Néel state is $0.17=(0.895)^{16}$. We conclude that, independent of the nature of the long-ranged order, the short-ranged correlations in even this simplest of Heisenberg models are remarkably well captured by the NN-RVB state.

(2) The ground states exhibit a great deal of wave-function "rigidity." Over a fair range of couplings away from the corners of the phase diagram [see Fig. 2(b)] where they are by definition the exact ground state, the overlap between $|SDW_i\rangle$, and the true ground state remains close to one [see Fig. 3(b)]. We identify these regions of the phase diagram as being approximately the regions where, in the thermodynamic limit, the ground state has a broken symmetry of the indicated SDW kind.

(3) We have verified our identification of the various SDW phases by evaluating the spin-spin correlation functions

$$G(\mathbf{R}-\mathbf{R}')=\langle \mathbf{S}_R\cdot\mathbf{S}_{R'}\rangle \tag{3}$$

as a function of J_i (see Fig. 4). In all cases, in the corners of the phase diagram, the spin-spin correlation function corresponds to the states represented in Fig. 1.

(4) We have also calculated the appropriate susceptibilities,

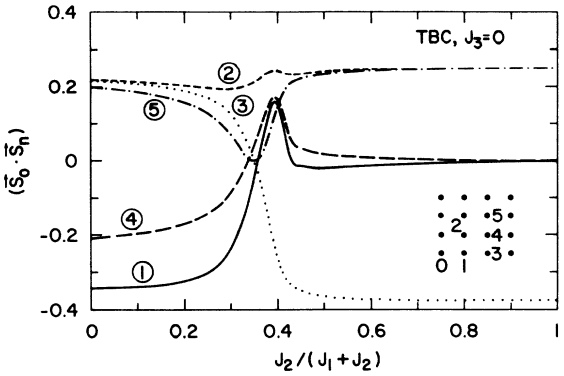

FIG. 4. Spin-spin correlation functions along the line $J_3=0$. The curves labeled 1–5 are, respectively, the correlation function evaluated for the first through fifth nearest-neighbor spins. Note that for large J_2, the correlation function looks much like the correlation function for $J_2=J_3=0$, but on the single sublattice of Fig. 2(b). There is almost no correlation between the spins on different sublattices over most of the region where the overlap with SDW_2 is large.

$$\chi_j=\sum_{n\neq 0}\frac{|\langle 0|s_{Q_j}|n\rangle|^2}{E_n-E_0}\ , \tag{4}$$

where s_Q is the Fourier transform of $\mathbf{S}_R$, n is summed over all (spin-1) excited states, j labels the appropriate SDW state, and $\mathbf{Q}_1=(\pi,\pi)$ and $\mathbf{Q}_2=(\pi,0)$. χ_j for $J_3=0$ is shown in Fig. 5. The susceptibility χ_j is large wherever the overlap with the corresponding SDW_j state is large (compare Fig. 3), and begins to fall when the overlap begins to fall.

(5) There is a large range of parameters near $J_1\sim J_2\sim J_3$ where the overlap of the exact ground state is small with all of the SDW states defined earlier [see Fig. 3(b)]; in what follows we will argue that this is a region with a non-SDW ground state. In part of this region, the overlap with the NN-RVB is large (>0.95), and, in fact, larger than with any of the SDW states [see Fig. 3(c)]. We suggest that in this region there exists a phase with a

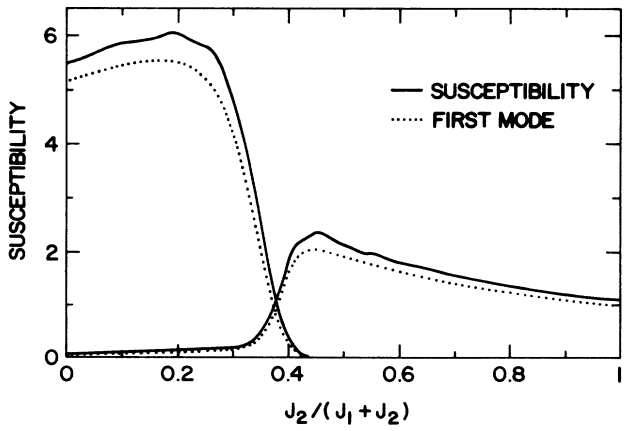

FIG. 5. The susceptibilities (solid line) and their first mode approximations (dotted line) for the SDW_1 and SDW_2 states for $J_3=0$ and TBC's. See Eq. (4) in the text.

SR-RVB ground state. The maximum overlap with the NN-RVB along the $J_3=0$ line is 0.995 and occurs at $J_1:J_2:J_3=1:0.37:0$, just beyond the point where linear spin-wave analysis predicts the disappearance of Néel order.[24] At this point, the expectation value of the Klein Hamiltonian in the exact ground state is $(0.01)J$ per site. [Note that the overlap with SDW_1 is still large (~ 0.95) at this point; for this reason, when we discuss the properties of a representative point in the non-SDW ("liquid") phase, we have chosen the point $J_1:J_2:J_3=1:0.61:0$, where the overlap with NN-RVB is still moderate, 0.47, and the expectation value of the Klein Hamiltonian is still small, 0.1 per site, while the overlap with SDW_1 is relatively smaller, 0.30.]

(6) We have computed the excitation spectrum in both the spin-0 and spin-1 sectors as a function of J_i. The excitation energies of the six lowest-lying spin-0 and six lowest-lying spin-1 states are shown as a function of J_2/J_1 along the line $J_3=0$ in Fig. 6(a). A more complete spectrum for different values of J_i is shown in Figs. 6(b)–6(g): Figures 6(b) and 6(c) are for the nearest-neighbor Heisenberg model ($J_1:J_2:J_3=1:0:0$), Figs. 6(d) and 6(e) are for $J_1:J_2:J_3=1:0.61:0$, and Figs. 6(f) and 6(g) are for $J_1:J_2:J_3=1:0.29:0.23$; Figs. 6(d)–6(g) are in the putative SR-RVB region.

(a) In the regions we have identified as SDW phases, there is always one (or, in the case of SDW_2 and SDW_3, two and four, respectively) anomalously low-energy spin-1 excited state which transforms under translations in the same way as the expected SDW state. Thus, for instance, in the SDW_1 region, the lowest-lying excited state is a spin-1 state with $\mathbf{k}=(\pi,-1)$ [analogous to $\mathbf{k}=(\pi,\pi)$ for PBC's]. Moreover, for each value of $\mathbf{k}$, the lowest-lying spin-1 excited state has energy substantially below that of the next lowest states, while the higher-lying states appear to form a continuum. By contrast, the lowest-lying

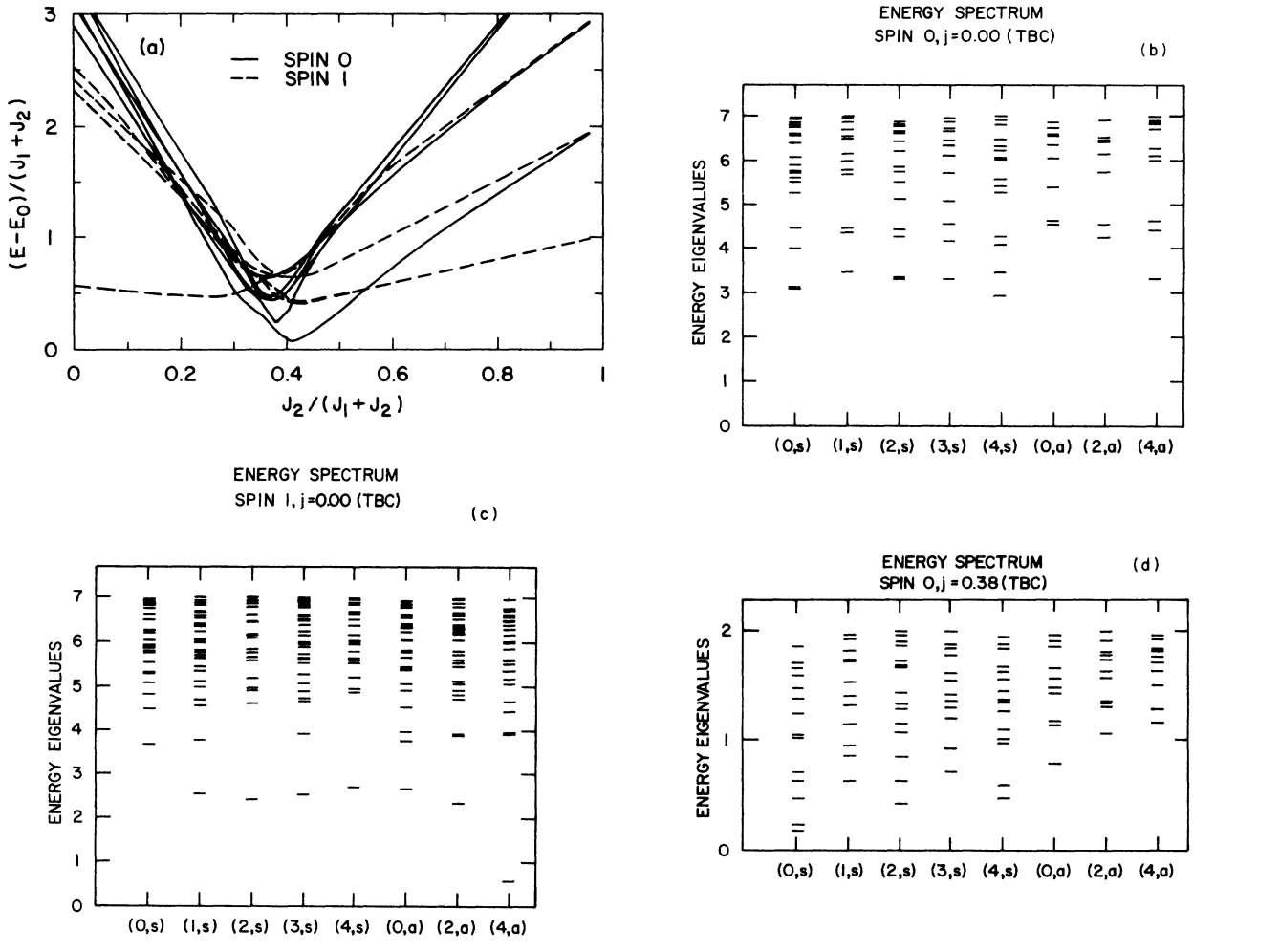

FIG. 6. (a) The energies of the lowest six spin-0 (solid lines) and the lowest six spin-1 (dashed lines) excited states along the line $J_3=0$ with TBC's (b) and (c). The spin-0 and spin-1 excitation spectra for $J_2=J_3=0$ (SDW_1 region). The system has TBC's and the symmetry of the states is labeled accordingly. k is essentially the crystal momentum in the x direction. The spectrum is symmetric under $k\rightarrow -k$, so we have only shown the states for positive k. (d) and (e) The excitation spectrum for $J_1:J_2:J_3=1:0.61:0$ (putative SR-RVB region) plotted in the same way as in (b) and (c). (f) and (g) The excitation spectrum for $J_1:J_2:J_3=1:0.29:0.23$ (putative SR-RVB region) plotted in the same way as in (b) and (c). In (d)–(g), $j=J_2/(J_1+J_2+J_3)$ and $jj=J_3/(J_1+J_2+J_3)$.

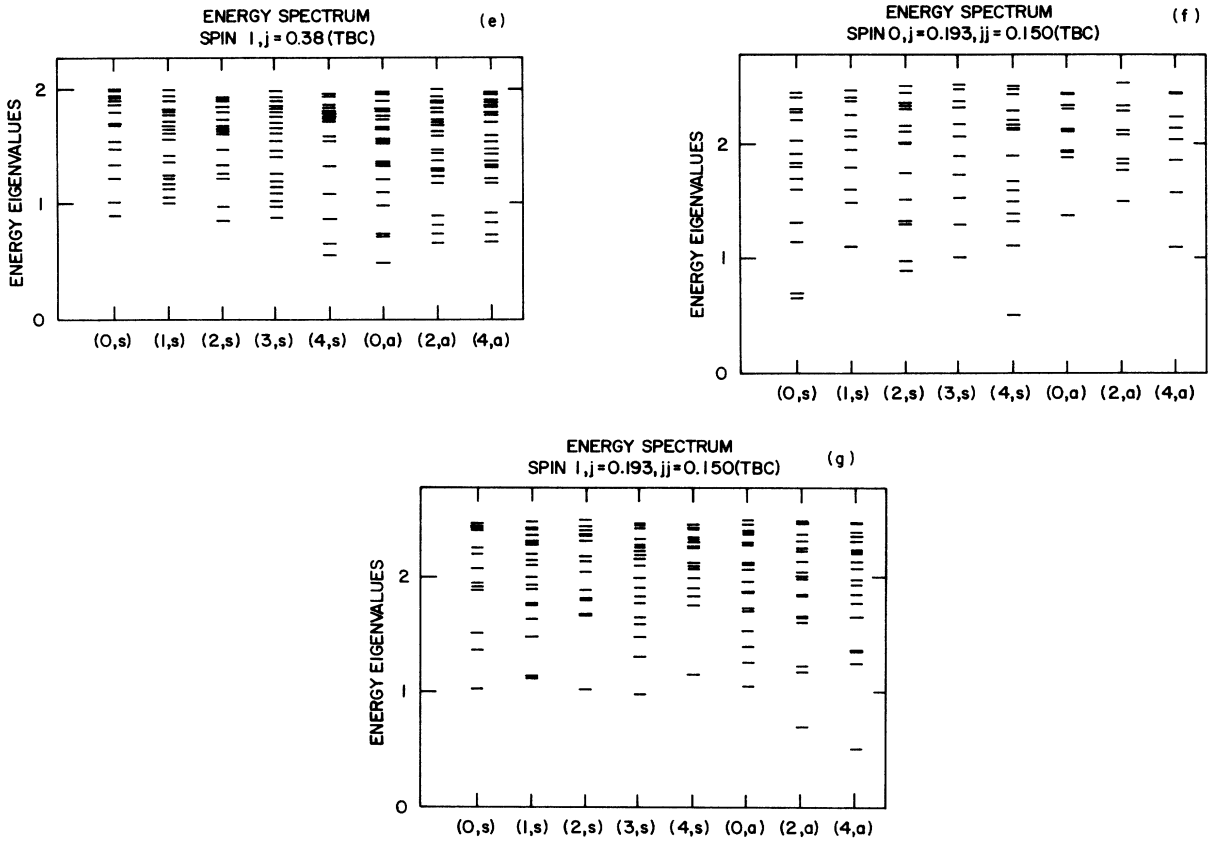

FIG. 6. (*Continued*).

spin-0 excited states are considerably higher in energy than the corresponding spin-1 states and all lie at what appears to be the bottom of a continuum. This is the expected finite-size behavior of a system which will exhibit broken spin-rotational symmetry in the thermodynamic limit. The anomalously low-lying spin-1 excited state indicates the nature of the emerging SDW order. A state with finite sublattice magnetization is necessarily an admixture of (at least) a spin-0 and a spin-1 state, so a low-lying spin-1 state is an obvious indicator of a tendency toward SDW order. [Indeed, as shown by the dotted curve in Fig. 5, the susceptibility in the SDW phases is well approximated by the single-mode approximation (SMA) in which the sum in Eq. (4) is replaced by the single term corresponding to the lowest-lying spin-1 excited state.] In the thermodynamic limit, the broken-symmetry state will have a branch of gapless magnon excitations, i.e., the Goldstone boson corresponding to the broken spin-rotational symmetry.

We thus identify the branch of isolated spin-1 excitations at other values of $\mathbf{k}$ as the one-magnon excitations, and the band of higher-energy states as the bottom of the spin-1 sector of the two-magnon continuum. Similarly, we identify the spin-0 excited states as the bottom of the spin-0 part of the two-magnon continuum. Notice the similarity between the spin-0 and spin-1 continua. Of course, in the thermodynamic limit, there will be no gap in either sector since the one-magnon creation energy must vanish at appropriate points in the Brillouin zone. However, we generally expect the finite-size effects to force the lowest-lying two-magnon state to higher energies than the lowest-lying one-magnon states, as is observed. It is important to note that in the regions which we have identified as non-SDW, we have found *no* anomalously low-lying spin-1 states.

(b) The energy spectrum looks rather different in the central region of the parameter space, which we have identified as the region with a non-SDW ground state. In this region, there is always a reasonably large gap to the lowest-lying spin-1 state; we view this as evidence that there is not still another SDW state that we have failed to identify. In fact, over much of this region, the energy gap to the lowest-lying spin-1 excitation is significantly *larger* than the gap to spin-0 excitations [see Fig. 6(a)]; At some points there are as many as six spin-0 excited states with lower energy than the lowest spin-1 state. The spectrum shown in Figs. 6(d) and 6(e) are fairly representative of the spectra in this region. The salient features of this spectrum are (i) there is no dramatic sign of a single-particle branch in the spectrum; both the spin-1 and the spin-0 spectra appear to be multiparticle continua, and (ii) the spin-1 and spin-0 spectra actually look fairly similar to each other, although the lowest-lying spin-0 states have noticeably lower energies. Like the ground state, the two lowest states are translationally invariant, $\mathbf{k}=(0,1)$.

(7) In the region in which the expectation value of the Klein Hamiltonian is small, we have calculated the over-

lap of the ground state with each individual valence-bond state, as well as with their equal-amplitude superposition (the NN-RVB state). The results are primarily interesting in the putative spin-liquid regime, as they provide a crude measure of whether the state is truly a spin-liquid state or actually a spin-Peierls or valence-bond crystal state. In a valence-bond crystal state, the overlap with the valence-bond states of appropriate broken symmetry (e.g., the "column" state or the "staggered" state) would be expected to be anomalously large. The results of this calculation, which require a certain amount of care to interpret, are discussed in Appendix B and partially summarized in Table II; for a representative point in this regime, $J_1:J_2:J_3=1:0.61:0$, the overlap with any of the obvious valence-bond crystal states is an order of magnitude smaller than the overlap with more "liquidlike" states. We take this as suggestive evidence that this regime is not a valence-bond crystal phase.

Beyond this summary, the results of our calculations are shown in the figures and described in the figure captions. These are an integral part of this paper, and the description is not repeated in the text.

B. Comparison with results for periodic boundary conditions

We have repeated the calculations in the spin-0 sector for PBC's as well. On the whole, the results are surprisingly similar to the results with TBC's. This increases our confidence that the systems we have studied are large enough to give meaningful information. Indeed, we consider it surprising that the differences between the two boundary conditions are as small as they appear to be.

In Fig. 7 we plot the energy of the ground state and four lowest-lying spin-0 excited states as a function of $J_2/(J_1+J_2)$ for TBC's (dashed line) and PBC's (solid line). Notice that the ground-state energies never differ by more than a couple of percent of (J_1+J_2). We feel this is remarkably small when we remember that for $J_1=0$, the gap to the one-magnon state, which is also a finite-size effect, is $0.57\,J_1$. We conclude that the ground state is particularly insensitive to finite-size effects, and

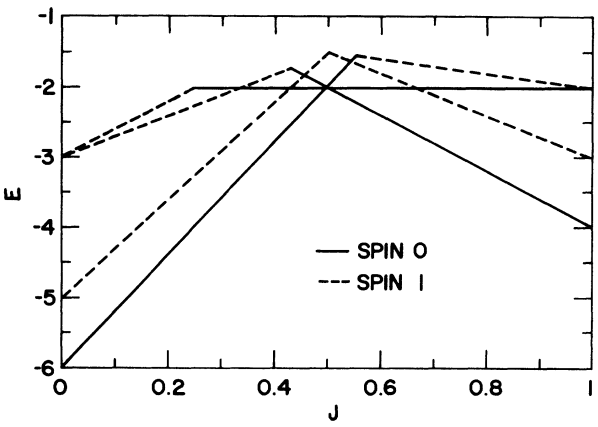

FIG. 8. The excitation spectrum of the lowest five states for the eight-site system with couplings appropriate to the PBC's. (See the description in Appendix A.) Spin-0 states are indicated by solid lines and spin-1 states by dashed lines.

that ground-state properties are closer to their thermodynamic values than might naively be imagined. This is further supported by the fact that for TBC, the fifth-neighbor spin-spin correlation in the J corner (see Fig. 4), has a value 0.20 which agrees remarkably well with the best Monte Carlo estimate[26] of the asymptotic value of this correlation function $0.15\pm.04$.

The low-energy spin-0 excited states are also rather insensitive to boundary conditions, except in the putative quantum spin-liquid region where the lowest-lying excited state for PBC's is anomalously low. For both choices of boundary conditions, the two lowest-energy states in the figure are translationally invariant ($\mathbf{k}=\mathbf{0}$) over the whole range of parameters. In Appendix B we show that such a boundary-condition-dependent anomalously low-lying state can occur in the quantum hard-core dimer model in its liquid phase. We are currently performing a more detailed study of the nature of the excited states in this regime to check whether this correspondence is correct. More generally, we feel that the near degeneracy of the ground state in the putative liquid phase for PBC's

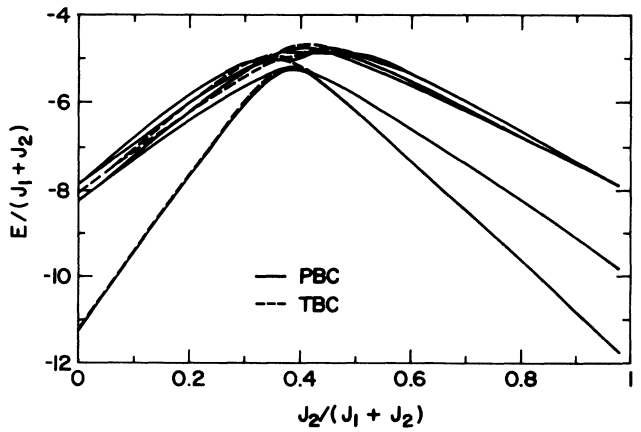

FIG. 7. The energy of the ground state and four lowest-lying spin-0 excited states as a function of $J_1/(J_1+J_2)$ for TBC's (dashed line) and PBC's (solid line).

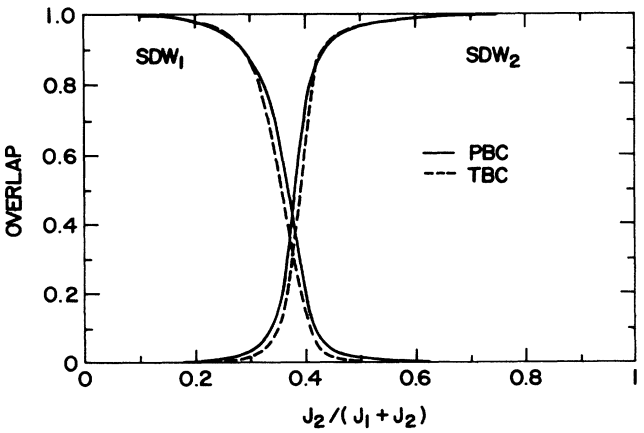

FIG. 9. The overlap of the ground state with the SDW_1 and SDW_2 states along the $J_3=0$ line for TBC's (dashed line) and PBC's (solid line).

with $J_3=0$ is due to the proximity of a point where the SDW_1, SDW_2, and the spin-liquid phases all coincide. Such a "triple point" occurs dramatically in the smaller, eight-site system (Appendix A and Fig. 8). This interpretation is consistent with the observation that for TBC, where the separation between the SDW_1 and SDW_2 phases is greater [see Fig. 3(a) and 3(b)], no such near degeneracy occurs. Moreover, for $J_3\neq 0$, the ground state is no longer nearly degenerate, even for PBC's. (Another possible explanation of the near degeneracy of the ground state for PBC's is that it reflects a true degeneracy of the ground state in the thermodynamic limit which arises due to the breaking of a discrete symmetry of order 2, such as time reversal. While this is a very intriguing possibility in light of a number of interesting suggestions[4] concerning the existence of such a broken symmetry, based on the results for TBC's and for PBC's with $J_3\neq 0$, we tentatively favor the interpretation previously outlined.)

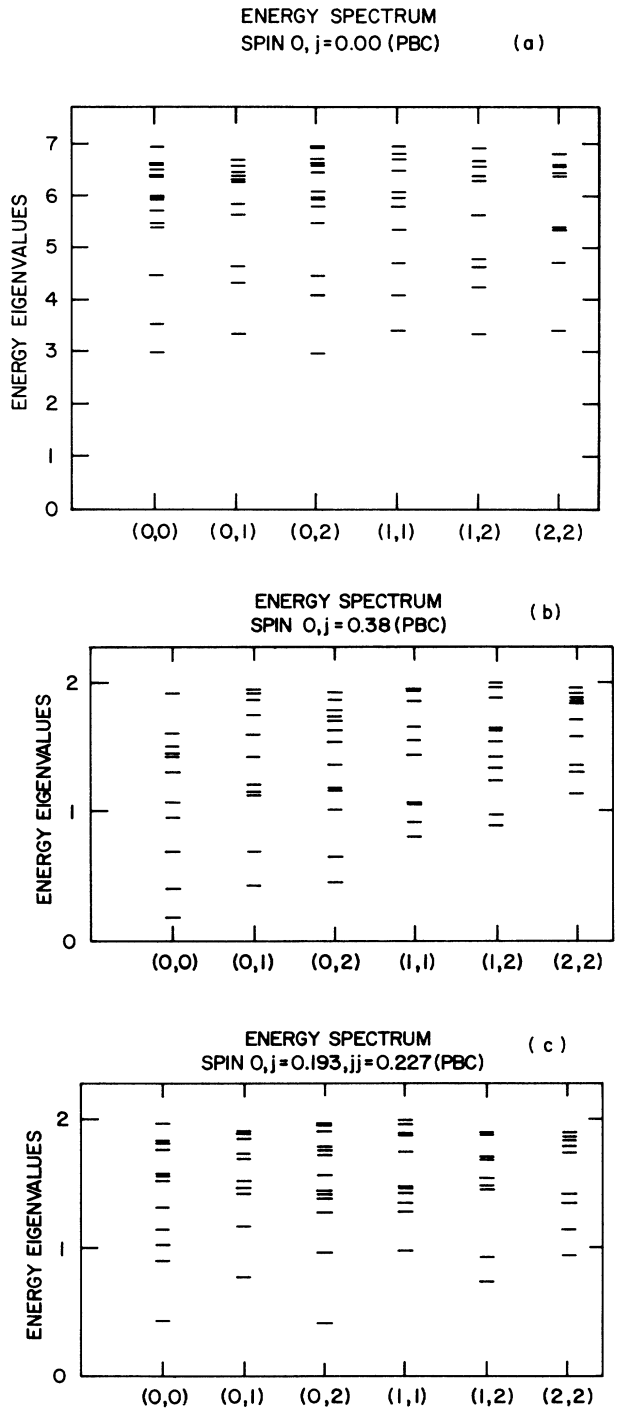

FIG. 10. The spin-0 excitation spectra for PBC's at three different points analogous to Fig. 6: (a) $J_2=J_3=0$ (SDW_1 region). (b) $J_1:J_2:J_3=1:0.61:0$ (putative SR-RVB region). (c) $J_1:J_2:J_3=1:0.33:0.39$ (putative SR-RVB region).

In Fig. 9 we compare the overlap with the SDW_1 and SDW_2 states along the $J_3=0$ line for TBC's and PBC's. Again, the plot shows a dramatic insensitivity of the ground state to boundary conditions. This insensitivity is much reduced at nonzero J_3; this is not surprising as the range of this interaction is half the size of the system, and the two boundary conditions imply different numbers of third neighbors. In comparing the results for nonzero J_3, we find that the differences between the two boundary conditions are considerably reduced if we rescale J_3 by the number of third neighbors, as already discussed. In Fig. 3(a), we show the contour map for the overlap with SDW for PBC's. [Compare the same plot for TBC's in Fig. 3(b).] In Fig. 10 we show the spin-0 spectrum at the analogous three points in the J_1-J_2-J_3 triangle as we showed in Fig. 6 for TBC's. As promised, all these figures show an increasing sensitivity to boundary conditions as J_3 is increased, but in no case do the boundary conditions have a dramatic effect.

IV. THEORETICAL INFERENCES

We have three primary theoretical inferences which we feel are supported by our numerical data. We list them along with a summary of the evidence which supports each conclusion. Each conclusion rests on the validity of the previous one and involves additional assumptions about the proper interpretation of the data. They are listed in order of increasing uncertainty. We stress that these are our best guesses as to the implications of our results.

(a) There exists a parameter range of the frustrated Heisenberg model which does not have an SDW ground state in the thermodynamic limit; the ground state does not spontaneously break spin-rotational symmetry. There is a large region of the phase diagram in which the overlap of the exact ground state with any of the obvious candidate SDW states is small. In this whole region, there is no anomalously low-lying spin-1 excited state, and the spin-spin correlation function is very short ranged. The computed susceptibility falls at roughly the same place that the overlap with the SDW trial states falls, implying that the decreasing overlap really does signal a transition to a new phase. Finally, a crude indicator of the effect of finite size on the extent of this intermediate regime can be obtained by comparing the results to the solution on a 2×4 lattice (see Appendix A). There, the "intermediate phase" occurs at a point where the energies of SDW_1 and SDW_2 cross. At the same coupling, a third state, presumably the intermediate (liquid) phase

ground state, becomes degenerate with the other two ground states. Thus, the region of intermediate phase apparently grows from a point for eight sites to a small interval for 16 sites.

(b) In the non-SDW region of the phase diagram, there exists a region in which the ground state is a liquid: The ground state does not have spontaneously broken translational symmetry (i.e., spin Peierls) order. The overlap with the equal amplitude NN-RVB is large in part of this region. We have explicitly checked the overlap of the exact ground state with each individual valence-bond state and find no evidence that any particular valence-bond state is preferred, as it would be in a valence-bond crystal. (We expand upon this point in Appendix B.) Moreover, the transition from the SDW to the non-SDW state appears to be continuous (second order), at least in some regions, as seen in the susceptibility curves in Fig. 5; a transition from an SDW to a spin-Peierls phase would be expected to be first order on symmetry grounds. Note, however, that for the 20°-curve in Fig. 3(d), there is a point at which the overlap with SDW_1 begins to drop smoothly, which we have identified as the transition from the SDW state to the liquid state, followed considerably later by a sharper drop, which seems to indicate a further, possibly first-order, transition. [This drop is more dramatic in the 20°-curve of Fig. 3(e), which shows the overlap with NN-RVB.] This further transition might either be a transition from the liquid state to a spin-Peierls state or from one liquid state to another (e.g., NN-RVB to second-neighbor RVB). Further evidence that in this region the ground state is liquid (as opposed to crystalline) comes from the absence of anomalously low-energy spin-zero excited states. If the system had spin-Peierls order in the thermodynamic limit, then for a finize-size system we would expect it to have three nearly gapless excited states of appropriate symmetry which herald the emerging broken translational and rotational symmetries. This is not found.

(c) In the liquid phase there exists a region where the overlap with the nearest-neighbor RVB state is large, and where the spectrum and correlation functions behave as expected of a SR-RVB state. This suggests that there ex-

TABLE I. Solution of the eight-site system. The eight-spin system has been split into sublattices A and B, each of which is further split into sublattices α and β. S indicates the total spin on the relevant sublattice and (S,S') indicates the pair of states $S\,S'$ and $S'S$; n is the degeneracy, E_1, E_2, and E_3 are the eigenvalues of the basic operators $(S_A+S_B)^2$, $S_{A^2}+S_{B^2}$, and $S_{A\alpha^2}+S_{A\beta^2}+S_{B\alpha^2}+S_{B\beta^2}$, respectively, that appear in H, and E_{PBC} and E_{TBC} are the energies of the $J_1=0$ 16-site system with PBC's and TBC's, respectively, where $J_3=J$ and $J_2=1-J$. Any entry in the table that is blank is the same as the entry immediately preceding it.

$((S_{A\alpha}S_{A\beta})$	$(S_{B\alpha}S_{B\beta}))$	(S_AS_B)	S_{A+B}	n	E_1	E_2	E_3	E_{PBC}	E_{TBC}
0 0	0 0	0 0	0	1	0	0	0	0	$-3J$
0 0	0 1	0 1	1	4	2	2	2	0	$-2J$
0 0	1 1	0 0	0	2	0	0	4	$-2J$	$-3J$
		0 1	1		2	2		$-J$	$-2J$
		0 2	2		6	6		J	0
0 1	0 1	1 1	0	4	0	4		$-2+2J$	$-2+J$
			1		2			$-1+J$	-1
			2		6			$1-J$	$1-2J$
0 1	1 1	0 1	1		2	2	6	$-2J$	$-2J$
		1 1	0		0	4		$-2+J$	$-2+J$
			1		2			-1	-1
			2		6			$1-2J$	$1-2J$
		1 2	1		2	8		$-3+4J$	$-3+4J$
			2		6			$-1+2J$	$-1+2J$
			3		12			$2-J$	$2-J$
1 1	1 1	0 0	0	1	0	0	8	$-4J$	$-3J$
		0 1	1	2	2	2		$-3J$	$-2J$
		0 2	2	1	6	6		$-J$	0
		1 1	0		0	4		-2	$-2+J$
			1		2			$-1-J$	-1
			2		6			$1-3J$	$1-2J$
		1 2	1	2	2	8		$-3+3J$	$-3+4J$
			2		6			$-1+J$	$-1+2J$
			3		12			$2-2J$	$2-J$
		2 2	0	1	0	12		$-6+8J$	$-6+9J$
			1		2			$-5+7J$	$-5+8J$
			2		6			$-3+5J$	$-3+6J$
			3		12			$2J$	$3J$
			4		20	12	8	$4-2J$	$4-J$

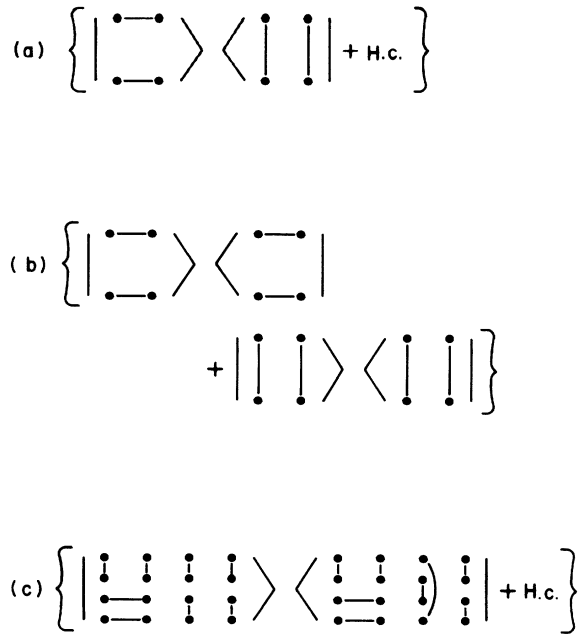

FIG. 11. Schematic representation of the terms in the dimer Hamiltonian: (a) is the pair-flip term on a plaquette, (b) is the dimer repulsion on a plaquette, (c) is the pair flip around the torus, and (d) is the dimer repulsion corresponding to (c).

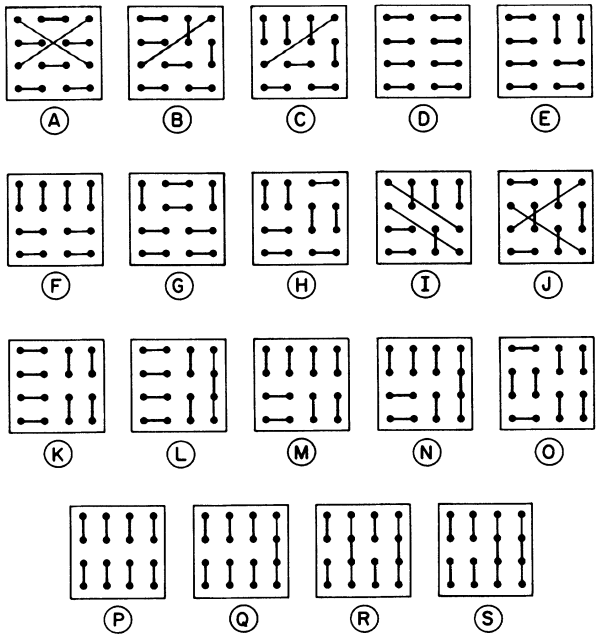

FIG. 12. The 19 independent dimer configurations on the system with TBC's. All other dimer configurations are related to these by symmetry. The letters labeling the configurations are used to refer to them in Table II.

TABLE II. Overlap with valence-bond states. Here we tabulate the overlap of the ground state for $J_1:J_2:J_3=1$: 0.61:0 with TBC, with the various valence-bond states shown in Fig. 12. The letters in the first column refer to the labels in the figure. The second column contains the sum of the squares of the overlaps with the pictured valence-bond state and all distinct valence-bond states that are related to it by symmetry. The third column lists the number of distinct valence-bond states related by symmetry. The fourth column lists the winding numbers of the corresponding dimer state, where the first entry refers to the twisted direction and the second to the periodic direction. The fifth column lists all other dimer configurations that can be obtained by a ring flip.

Dimer label	Overlap	Degeneracy related	Winding numbers	Ring flip
A	0.0115	2	(2,0)	
B	0.0309	32	(1,0)	
C	0.0351	32	(1,0)	
D	0.0755	2	(0,0)	
E	0.0907	16	(0,0)	
F	0.1150	16	(0,0)	
G	0.0508	16	(0,0)	
H	0.1043	16	(0,0)	
I	0.1093	16	(0,0)	
J	0.1008	16	(0,0)	
K	0.1820	8	(0,0)	*L*
L	0.1774	8	(0,1)	*K*
M	0.2311	16	(0,0)	*N,O*
N	0.2165	32	(0,1)	*M,O*
O	0.2133	16	(0,0)	*N,M*
P	0.5267	2	(0,0)	*Q,R,S*
Q	0.5010	8	(0,1)	*P,R,S*
R	0.4796	2	(0,2)	*P,Q,S*
S	0.4994	4	(0,0)	*P,Q,R*

ists a liquid phase which is adiabatically related to the nearest-neighbor RVB state, and which can reasonably be identified as a SR-RVB phase. The overlap with the NN-RVB state is large in the liquid region adjacent to the SDW_1 phase. Furthermore, the excitation spectrum shown in Figs. 6(d)–6(g) is qualitatively similar to what we expect for a SR-RVB state based on studies of the quantum hard-core dimer gas (which is a simplified model of the SR-RVB state): (i) The basic quasiparticle excitations appear to be massive (finite gap) spin-$\frac{1}{2}$ "spinons." Thus both the spin-1 and the spin-0 excitations are basically two-particle excitations and, if we ignore spinon-spinon interactions, are expected to be quite similar. This is consistent with the observed similarities between the spin-1 and spin-0 excitation spectra shown in Figs. 6(d)–6(g), and the fact that they are both dominated by what appear to be multiparticle continua. (ii) The lowest-lying excitations of the quantum hard-core dimer gas are[3] collective excitations, "resonons." As discussed in Appendix B, the low-lying spin-0 excited states in the spin-liquid regime can be interpreted as resononlike modes in a finite-size dimer gas.

V. CONCLUSIONS

We conclude with a few comments concerning the relation of the present results to the SR-RVB approach to high-temperature superconductivity. We have found evidence for the existence of a SR-RVB phase in a sufficiently frustrated Heisenberg model. While there is strong evidence derivable from a careful analysis[10] of experiments in La_2CuO_4 and $YBa_2Cu_3O_{6.5}$ that the undoped CuO plane is describable by a quasi-two-dimensional Heisenberg model with a SDW ground state (SDW_1), there are theoretical reasons[27,1] for believing that even low hole concentrations introduce a large amount of effective frustration into the model. Moreover, there is ample experimental evidence that doping levels as low as $x=2$–3 at.% in $La_{2-x}Sr_xCuO_4$ destroy the long-ranged SDW order. There is preliminary evidence[28] that above $x=5$ at. %, where the samples begin to be superconducting, the spin-spin correlation length is about 10–20 Å, or 2–5 lattice constants. Note that this is also roughly equal to the inferred[29] superconducting correlation length, $\xi_0 \sim 15$ Å. Thus, it seems reasonable to postulate that doping introduces sufficient frustration into the system to stabilize a SR-RVB state. The short correlation lengths are then easily understood, since for the NN-RVB state the spin-spin correlation length is estimated[11] to be about one to two lattice constants, while if fourth-neighbor valence bonds (the next-shortest valence bonds that connect different sublattices) are included, the correlation length is about seven lattice constants. It is hard to imagine any low-energy state of a Heisenberg model with dominantly nearest-neighbor antiferromagnetic exchange that has simultaneously such a short correlation length and correlations substantially different from the SR-RVB state. Of course, this may simply reflect the limits of our imagination.

A preliminary report of this work was presented previously.[30] We recently received copies of unpublished work by Hirsch and Tang[31] and by Dagotto and Moreo[32] which have some similar results.

ACKNOWLEDGMENTS

We would like to acknowledge useful discussions with E. Ramos, D. H. Lee, D. Huse, E. Rezayi, R. Singh, and S. Chakravarty. This work was supported in part by National Science Foundation (NSF) Grant Nos. PHY 85-07627 (M.R.) and DMR-87-06250 (S.S. and S.K.) A. K. was supported in part by the Swedish Natural Science Research Council.

APPENDIX A: ANALYTIC SOLUTION OF THE EIGHT-SITE SYSTEM

In this appendix, we solve the eight-site (2×4) system with twisted boundary conditions around the short direction and arbitrary J_1, J_2, and J_3 couplings; on a system this small, TBC's are essential to reproduce the nearest-neighbor coordination number (4) of the infinite lattice. The model can be solved analytically and is of interest for two reasons: It gives some insight into finite-size effects, and the 16-site (4×4) system at $J_1=0$ reduces to two noninteracting eight-site systems with particular values of the couplings.

The eight-site system with TBC's is easily solved because the nearest-neighbor J_1 couplings simply couple all the spins of one four-site sublattice (A) to all the spins of the remaining four-site sublattice (B). Calling the total spin on the sublattices $\mathbf{S}_A$ and $\mathbf{S}_B$, this part of the Hamiltonian can be written as

$$H_1=\tfrac{1}{2}J_1[(\mathbf{S}_A+\mathbf{S}_B)^2-\mathbf{S}_A^2-\mathbf{S}_B^2] .$$

To write the next-nearest and third-nearest neighbor interactions, we need to subdivide each four-site sublattice further into two-site subsublattices (α and β). Then, in an obvious notation, the total Hamiltonian is

$$\begin{aligned}H=&\tfrac{1}{2}J_1[(\mathbf{S}_A+\mathbf{S}_B)^2-\mathbf{S}_A^2-\mathbf{S}_B^2)\\&+\tfrac{1}{2}J_2[\mathbf{S}_A^2+\mathbf{S}_B^2-(\mathbf{S}_{A\alpha}^2+\mathbf{S}_{A\beta}^2+\mathbf{S}_{B\alpha}^2+\mathbf{S}_{B\beta}^2)]\\&+\tfrac{1}{2}J_3[(\mathbf{S}_{A\alpha}^2+\mathbf{S}_{A\beta}^2+\mathbf{S}_{B\alpha}^2+\mathbf{S}_{B\beta}^2)-6] .\end{aligned}$$

Here J_1 is the coupling to the ith nearest neighbor. (On a finite system, another possibility is to assign one J_1 coupling per minimal path to the ith nearest neighbor; this assignment reflects the coordination number of the infinite lattice.) The mapping of the 16-site problem with $J_1=0$ onto the eight-site problem is accomplished by expressing the eight-site J_1, J_2, and J_3 couplings in terms of the 16-site couplings as follows: $(J_1,J_2,J_3)_8=(J_2,J_3,0)_{16}$ for PBC's on the 16-site lattice, and $(J_1,J_2,J_3)_8=(J_2,J_3,J_3)_{16}$ for TBC's on the 16-site lattice. Note that for TBC's on the 16-site lattice, the alternative assignment of couplings is *not* just a rescaling. Our solution is given in Table I.

Though the table is the complete solution, it is not particularly illuminating. We plotted all the energy eigenvalues for the two special cases that correspond to the $J_1=0$ 16-site system (Fig. 8 for the five lowest states in the PBC case) and found the following interesting

features: (1) For both systems, the ground state is always a spin-0 state that switches abruptly from one SDW state to the other as J varies, and is degenerate with a third spin-0 state at the transition. Thus, in the ground state, the "liquid phase" has shrunk to a point. This suggests that the liquid phase is not a finite-size artifact, but on the contrary, becomes more evident as the size of the lattice increases. (2) The excited spectra are analogous to the spectra on the full 16-site lattice: For the system that corresponds to PBC's on the 16-site system, for J well away from the "phase transition" (the switch in the ground state), the first excited state is a spin-1 state (a magnon), but near the transition, the lowest excited states are spin-0 states. For the other system, the situation is similar except that the states are more degenerate. In particular, for $J > J_c$, the ground state is fourfold degenerate; we believe this merely reflects the small size of the system and the small number of interactions.

APPENDIX B: RELATION OF THE SPIN-LIQUID STATE TO THE DIMER MODEL

In Ref. 3 it was pointed out that the states in the nearest-neighbor valence-band subspace of a spin-$\frac{1}{2}$ Heisenberg model are in one-to-one correspondence with the states of a hard-core quantum dimer gas on the same lattice: The dimer states are orthogonalized versions of the corresponding valence-bond states. Thus, to the extent that the low-lying states of frustrated spin system lie in the nearest-neighbor valence-bond subspace, the system is approximately equivalent to a dimer gas. It was further argued in Ref. 3 that the effective dimer Hamiltonian has short-range interactions, and certain properties of an ultra-short-ranged version of this model were derived. In this appendix we compare in gross terms the expected behavior of the dimer model on a 4×4 lattice with appropriate boundary conditions to the ground-state and low-lying excited spin-0 states of the frustrated Heisenberg model in the putative spin-liquid regime. The results, while preliminary, are highly suggestive. We intend to carry out a more extensive comparison at a future date.

1. The quantum-dimer model

The quantum-dimer model is a Hamiltonian which operates on the (orthonormal) dimer states. We consider here the shortest-range model (shown schematically in Fig. 11) which consists of a sum of all terms which operate on a pair of adjacent dimers. The first two terms in the Hamiltonian are the same as the model discussed in Ref. 3: The pair-flip operator (with coupling J) flips a pair of parallel dimers on a plaquette from horizontal to vertical or vice versa [Fig. 11(a)]. The nearest-neighbor dimer repulsion (with coupling V) counts the number of plaquettes which have a pair of parallel dimers [Fig. 11(b)]. For the small systems we have considered, there are two other comparably short-ranged interactions which also involve a pair of dimers, in this case arranged along a single closed line around the effective torus (in the periodic direction for TBC's and in either direction for the PBC's): The ring-flip operator (with coupling J') flips a pair of dimers along such a ring which circles the system [Fig. 11(c)], and a potential energy term (with coupling V') which counts the number of such rings which are tiled by dimers [Fig. 11(d)]. We can define a winding number in the dimer state space as in Ref. 3, in which case the J' term changes the winding number by one, whereas all the other terms leaving the winding number invariant. The analogs of J' and V' in the thermodynamic limit are exponentially small interactions involving cooperative ring exchange of dimers along rings that enclose the entire system. We have not included a ring-exchange term in the Hamiltonian involving resonances between dimer configurations which have different winding numbers in the twisted direction, such as between configurations A and D in Fig. 12; such terms are longer-range interactions involving the motion of at least four dimers. In our view, the absence of resonance terms in the twisted direction is the primary reason that the results for TBC's differ from those for PBC's in the liquid phase (see the discussion following).

The various terms in the model favor different sorts of ground states. Large V favors a valence-bond-crystal ground state; for V positive a "staggered" state, such as A in Fig. 12 is favored while negative V favors a "column state" such as D or P in the figure. J favors resonance between different configurations in the same winding number sector, such as M and P in Fig. 12; J thus favors a more liquidlike state. J' and V' are analogous to J and V in that J' favors a resonating liquidlike state with comparable amplitude on configurations such as P, Q, R, and S, while V' favors various specific single dimer configurations.

As noted in Ref. 3, a special coincidence occurs for $V=J$ and J' and V' equal zero (and, by analogy, for $V'=J'$ and J and V equal zero): The ground state is severalfold degenerate and each ground state consists of an equal amplitude superposition of all dimer configurations which are connected to a given seed configuration by repeated pair flips, i.e., all configurations with a given winding number (see Table II). For V slightly less than J, these ground states cease to be degenerate; the energy of each state is equal to $-(J-V)$ times the average number of nearest-neighbor dimer pairs (plaquette "flipables") in the original ground state. By analogy, for $J'=V'$, the ground state is highly degenerate with each ground state consisting of an equal amplitude superposition of all dimer configurations which are related to a given seed by repeated ring flips (see Table II). Similarly, for V' slightly less than J', the degeneracy is lifted, and the energy of each of these ground states becomes $-(J'-V')$ times the average number of ring flipables in that state.

2. Ground-state correlations at $J_1:J_2:J_3=1:0.61:0$ with TBC's

We have computed the overlap between the ground state and the various individual valence bond states for $J_1:J_2:J_3=1:0.62:0$ with TBC's. The result is shown in Table II for 19 representative valence-bond states, where the numbers refer to the valence bond states pictured in Fig. 12. All other valence-bond states are related to these

19 by some symmetry of the lattice. In the table we also list the number of distinct valence-bond states related by symmetry to the pictured state, the winding numbers of the dimer configuration, and which dimer configurations are connected by a ring flip around the periodic direction. Note that the sum of the squares of the amplitudes is significantly greater than 1; this is a consequence of the nonorthogonality of the different valence-bond states.

We observe that the overlap with the pure valence-bond crystal states, A and D, are significantly suppressed relative to more liquidlike states. This supports the thesis that the state here is not a valence-bond crystal. Note, however, that configuration P, which looks like a rotated version of D, is one of the configurations with maximum overlap. We understand this result by noting that all the configurations (P,Q,R,S) which are related to P by a ring flip have almost equal amplitude (to within 5%). Moreover, in each multiplet of states that are related to each other in this way, notably (I,J), (K,L), and (M,N,O), the same observation applies. This can be understood in the dimer model if we suppose that J' and V' are the largest interactions and V' is slightly less than J'. Moreover, the multiplets of states have amplitudes which scale roughly with the average number of ring flipables in each set: (I,J) has one, (K,L) and (M,N,O) have two and (P,Q,R,S) has four. We can estimate the relative size of the effective interactions J and J' by noting that the amplitude in P is roughly twice the amplitude in M, so $J \sim (J'-V')$. The smallness of the amplitudes of the configurations A, B, and C, which have nonzero winding number in the twisted direction, supports the assumption that longer-range dimer interactions are negligible.

Since the ring flip is so important, it is easy to understand why the excitation spectrum is different for the TBC's and the PBC's in this regime. Unfortunately, this result also emphasizes the fact, implicit already in the difference between the two boundary conditions, that the result could be significantly affected by finite-size effects. Nonetheless, we find that the suppression of the pure valence-bond crystal states, and the fact that resonance of both the plaquette and the ring varieties are the dominant interactions, provide strong evidence that any tendency of the system to form a valence-bond crystal is rather weak, and corroborative, although circumstantial evidence, that the ground state is a spin liquid.

*Current address: Department of Physics, UCLA, Los Angeles, California.

†Current address: Department of Physics, University of California, Berkeley, CA 94720.

[1]P. W. Anderson, Science **235**, 1196 (1987); G. Baskaran, Z. Zou, and P. W. Anderson, Solid State Commun. **63**, 973 (1987); P. W. Anderson, G. Baskaran, Z. Zou, and T. Hsu, Phys. Rev. Lett. **58**, 2790 (1987).

[2]S. A. Kivelson, D. S. Rokhsar, and J. P. Sethna, Phys. Rev. B **35**, 8865 (1987); Europhys. Lett. **6**, 353 (1988).

[3]S. A. Kivelson and D. S. Rokhsar, Physica C **153-155**, 531 (1988); D. S. Rokhsar and S. A. Kivelson, Phys. Rev. Lett. **61**, 2376 (1988).

[4]V. Kalmeyer and R. B. Laughlin, Phys. Rev. Lett. **59**, 2095 (1987); R. B. Laughlin, *ibid.* **60**, 2677 (1988); Science **242**, 525 (1988); (unpublished). See also E. J. Mele, Phys. Rev. B **38**, 8940 (1988). For a more general discussion of T and P violating spin-liquid states see X. G. Wen, F. Wilczek, and A. Zee, Phys. Rev. B **39**, 11 413 (1989).

[5]M. Kohomoto and Y. Shapir, Phys. Rev. B **37**, 9439 (1988); M. Kohomoto, *ibid.* **37**, 3812 (1988); P. L. Iske and W. J. Caspers, Physica A **142**, 360 (1987).

[6]I. Affleck and J. B. Marston, Phys. Rev. B **37**, 3774 (1988); J. B. Marston and I. Affleck, *ibid.* **39**, 11 538 (1989); G. Kotliar, *ibid.* B **37**, 3664 (1988); A. Ruckenstein, P. Hirschfeld, and J. Appel, *ibid.* **36**, 857 (1987).

[7]C. Gros, R. Joynt, and T. M. Rice, Z. Phys. B **68**, 425 (1988).

[8]J. Otima and D. D. Betts, Can. J. Phys. **56**, 897 (1978).

[9]J. D. Reger and A. P. Young, Phys. Rev. B **37**, 5978 (1988); D. A. Huse and V. Elser, Phys. Rev. Lett. **60**, 2531 (1988); D. A. Huse, Phys. Rev. B **37**, 2380 (1988).

[10]S. Chakravarty, B. I. Halperin, and D. Nelson, Phys. Rev. Lett. **60**, 1057 (1988).

[11]S.-D. Liang, B. Doucot, and P. C. Anderson, Phys. Rev. Lett. **61**, 365 (1988).

[12](a) I. Affleck, T. Kennedy, E. H. Leib, and H. Tasaki, Phys. Rev. Lett. **59**, 799 (1988); (b) Commun. Math. Phys. **115**, 477 (1988); (c) see also D. P. Arovas, A. Auerbach, and F. D. M. Haldane, Phys. Rev. Lett. **60**, 531 (1988). Actually, the existence of a gap was only proved in one dimension. Exponential decay of correlations was proved for a two-dimensional model in (b), which we take to be very strong evidence for the existence of a gap.

[13]P. W. Anderson, Mater. Res. Bull. **8**, 153 (1973); P. Fazekas and P. W. Anderson, Philos. Mag. **30**, 432 (1974); B. Sutherland, Phys. Rev. B **37**, 3786 (1988).

[14]L. Pauling, *The Nature of the Chemical Bond* (Cornell University Press, Ithaca, 1960).

[15]D. S. Rokhsar (unpublished).

[16]S. A. Kivelson and D. S. Rokhsar, Phys. Rev. Lett. **61**, 2630 (1988); V. Kalmeyer and R. B. Laughlin, *ibid.* **61**, 2631 (1988).

[17]L. B. Ioffe and A. I. Larkin, Int. J. Mod. Phys. B **2**, 203 (1988); Phys. Rev. B **37**, 5730 (1988).

[18]D. Huse (private communication).

[19]P. Wiegmann, Phys. Rev. Lett. **60**, 821 (1988); (unpublished).

[20]D. J. Klein, J. Math. Phys. A **15**, 661 (1982).

[21]J. Chayes, L. Chayes, and S. A. Kivelson, Commun. Math Phys. **123**, 53 (1989).

[22]F. D. M. Haldane, in *The Quantum Hall Effect,* edited by R. Prange, and S. Girvin (Springer-Verlag, New York, 1987), p. 303.

[23]W. Marshall, Proc. R. Soc. London, Ser. A **232**, 48 (1955).

[24]S. Chakravarty, B. I Halperin, and D. Nelson, Phys. Rev. B **39**, 2344 (1989); P. Chandra and B. Doucot, *ibid.* **38**, 9335 (1988).

[25]S. Tang and H. Q. Lin, Phys. Rev. B **38**, 6863 (1988).

[26]J. D. Reger, J. A. Riera, and A. P. Young, (unpublished). See also Ref. 11.

[27]Y. Nagaoka, Phys. Rev. **147**, 392 (1966); M. Inui, S. Doniach, and M. Gabay, Phys. Rev. B **38**, 6631 (1988).

[28]R. Birgeneau *et al.*, Phys. Rev. B **38**, 6614 (1988); **39**, 2868 (1989).

[29]See, for example, A. Kapitulnik, Physica C **153**, 520 (1988).

[30]S. Sondhi, F. Figueirido, A. Karlhede, S. Kivelson, and M. Rocek, Bull. Am. Phys. Soc. **33**, 558 (1988).

[31]J. E. Hirsch and S. Tang, Phys. Rev. B **39**, 2887 (1989).

[32]E. Dagotto and A. Moreo, Phys. Rev. Lett. **63**, 2148 (1989).